BENEFITS OF LATERAL STRENGTH IN TERMS OF RESIDUAL CAPACITY

M. Raghunandan(1), S.J. Welsh-Huggins(2), A.B. Liel(3)

(1) *Assistant Professor, Dept. of Civil Engineering, IIT Bombay, India, meerar@iitb.ac.in*
(2) *Ph.D. Candidate, Dept. of Civil, Environmental and Architectural Engineering, University of Colorado Boulder, sarah.welshhuggins@colorado.edu*
(3) *Associate Professor, Dept. of Civil, Environmental and Architectural Engineering, University of Colorado Boulder, abbie.liel@colorado.edu*

Abstract

This paper investigates how altering design lateral strength may benefit the post-earthquake residual capacity of a structure. Lateral strength is a key design variable, yet its impact on residual capacity is not well-understood. Residual capacity quantifies the ability of an earthquake-damaged structure to resist collapse in subsequent earthquake events such as aftershocks, which impacts post-earthquake occupancy decisions such as building tagging. Here, the residual capacity is assessed for a set of 4-story modern U.S. reinforced concrete moment frames seismically designed with different design base shears, *i.e.* varying lateral strength levels. Other characteristics of the frames, such as deformation capacity, do not vary significantly. The collapse resistance of each structure in both intact and damaged states is assessed through incremental dynamic analysis, using a set of ground motions representative of California seismicity. Each structure's residual capacity is assessed for multiple damage states, representing different levels of damage from the mainshock (first earthquake) event. Collapse fragility assessments are used to quantify a structure's ability to resist further earthquake damage, based on residual capacity remaining in a structure after an earthquake. The results show that the stronger (above-code) buildings exhibit the same relative decrease in collapse capacity for a given damage state, but are stronger than the code and below-code counterparts in both intact and damaged configurations. In addition, the stronger buildings are likely to experience less damage and, therefore, experience smaller reductions in residual capacity in a given shaking event. These results can be used to link building design strength to target desired post-earthquake outcomes.

Keywords: design strength; collapse capacity; residual capacity; reinforced concrete frames; aftershocks

1. Introduction

Lateral strength is perhaps the most fundamental of seismic design variables. It is well-documented (*e.g.* [1]) and intuitive that increases in strength produce better seismic performance, all factors (particularly deformation capacity) being similar equal. It is also evident that stronger buildings generally require larger material volumes, which can increase upfront construction costs [2]. Likewise, there is a body of literature that examines the aftershock performance of various types of buildings with different levels of damage (*e.g.* [3], [4]), showing somewhat increased risk of damage and collapse if the potential for aftershocks is considered [5]. Yet, it is not clear how simple decisions about design strength impact post-earthquake, or residual, capacity. Residual capacity is defined here as the capacity of an already-shaken structure to resist collapse under subsequent shaking. The concept of residual capacity is thus central to procedures for building tagging [6] and other post-earthquake occupancy decisions [7]. After an earthquake, the decision-making environment is complicated by varying perspectives from many actors – building owners, government and insurance providers, among others – and the potential for aftershocks that may further impact already damaged buildings (*e.g.* [8], [9]). For example, after the series of earthquakes that struck Christchurch, New Zealand, this complexity contributed to a large number of multistory commercial buildings, which were mostly reinforced concrete, being demolished [10]. While some of these structures were severely damaged, others were less so, and it is likely that the large number of demolished buildings and delays in making decisions about whether to demolish further slowed Christchurch's recovery, potentially impairing the community's seismic resilience. The concept of residual capacity and the uncertainty about buildings' residual capacities were key factors in determining whether structures were demolished or repaired. The Christchurch experience points to the importance of developing methods for assessing the residual capacity of a structure, and for examining design decisions that may positively impact this capacity.

This paper investigates how changes to design strength can improve post-earthquake outcomes in the context of residual capacity. To do so, we assess a group of seismically-designed reinforced concrete moment frame structures that differ only in terms of lateral strength. All structures meet modern U.S. seismic design criteria for high seismic areas (*e.g.* California) [1], [11], but with varying design base shears, and accordingly different lateral strength levels. To quantify the impact of these design changes, we assess the collapse resistance of each intact structure using incremental dynamic analysis [12], wherein structures are subjected to a set of ground motions representative of seismicity for the assumed site of interest. Subsequently, the collapse resistance of earthquake-damaged structures is assessed, again through incremental dynamic analysis, following approaches developed by Raghunandan *et al.* [4]. Collapse fragility assessments of the intact and damaged structures are then used to quantify the residual capacity. Each structure's residual capacity is assessed considering multiple damage states, enabling consideration of different levels of damage the intact structure experiences during the mainshock or first earthquake event.

2. Buildings investigated

This study investigates the relationship between a building's design strength and its post-earthquake residual capacity using seven commercial buildings designed for southern California. The design of these modern four-story office buildings is adopted from Haselton *et al.* [1]. Each building has a floor area of 120 ft. by 180 ft. Space frames are designed with six reinforced concrete (RC) frame lines resisting lateral loads in each direction. Perimeter frames are designed such that the exterior (perimeter) frame lines carry lateral loads and interior columns are gravity-load bearing only. The height of the first story is 15 ft., while all others are 13 ft; bay width is 30 ft. The buildings are assumed to be located at a Los Angeles site in seismic design category D [13]. This site has a design spectral acceleration for short periods (S_{DS}) of 1.0g and at 1s (S_{D1}) of 0.6g.

Each building was designed to be code-conforming in all respects, except design strength. The building designs differ in terms of the so-called "R factor", which is an inverse modifier on structural strength in the design process [13], *i.e.* strength is proportional to 1/R. ASCE 7-10 [13] specifies a value of R = 8 for special RC frames. Here, we first examine the space and perimeter frame buildings designed for this code-specified value. The space frame structure is also assessed for stronger (R < 8) and weaker (R > 8) variations. A below-code (weaker) variation of the perimeter frame is considered in addition to the code-conforming version. Design for lower R factors require larger member sizes and increased amounts of reinforcing steel to satisfy the higher strength requirements. The larger member sizes also make the stronger models stiffer than their code-compliant and below-code counterparts, producing smaller fundamental periods for the above-code buildings. The opposite trend is observed for the weaker buildings. Table 1 presents the structural member dimensions and design details for the buildings. Perimeter frame design is more heavily governed by lateral load than space frame design so changes in design base shear have a more direct influence on member sizes and design than for the the space frames.

Table 1– Building design information.

Building ID	**R**	**Frame Type**	**Design Base Shear**[1] (kips)	**Time Period (T_1)**[2] (s)	**Ductility**[3] **(μ^T)**	**Column Size** (b x h; in x in)	**Beam Size** (b x h; in x in)
2001	4	Space	386	0.74	10.5	30 x 30	30 x 36 (floors 1-2); 30 x 30 (floors 3-4)
2020	5.3	Space	290	0.78	12.6	30 x 30	30 x 34 (floors 1-2); 30 x 28 (floors 3-4)
1010	8	Space	193	0.86	10.6	30 x 30	30 x 30 (floors 1-2); 30 x 24 (floors 3-4)
2022	10	Space	156	0.92	10.2	28 x 28	28 x 28
2003	12	Space	129	0.97	10.3	28 x 28	28 x 28 (floors 1-2); 28 x 26 (floors 3-4)
1009	8	Perimeter	580	1.16	12.5	34 x 30 (corners), 38 x 30 (center)	34 x 30 (all floors)
2052	12	Perimeter	386	1.15	16.9	30 x 30 (corners), 36 x 30 (center)	30 x 34 (all floors)

[1]Design base shear: design base shear per seismic frame in units of kips
[2]Time period from eigenvalue analysis of simulation models (Section 3), considering cracked section properties.
[3]Period based ductility capacity as determined from nonlinear static pushover analysis [14].

3. Nonlinear models

The OpenSEES software [15] was used to conduct nonlinear analysis of two-dimensional, three-bay models of each of the buildings of interest. Beams and columns are modeled as elastic beam-column elements with plastic hinges at the ends to capture the nonlinear response. The hinges are assigned a material model developed by Ibarra *et al.* [16]. The hinge material model has a trilinear monotonic backbone and stiffness and strength degradation rules such that it is capable of capturing strain softening at large deformations associated with concrete spalling and rebar buckling. In addition, the material model is capable of representing multiple mechanisms of cyclic strength and stiffness deterioration [16]. The properties of the hinges are calibrated to experimental results of over 250 concrete columns using equations developed by Haselton *et al.* [17], such that modeling parameters, especially deformation capacity and degradation, considers differences in design and detailing between different structural components. The buildings were modeled with 5% damping, with Rayleigh damping in the first and third modes and assigned only to the models' elastic elements. The beam-column joints are modeled with an elastic spring. More details about the modeling are provided in Haselton *et al.* [1]. The models also have a leaning (P-Δ) column to carry gravity loads that are part of the seismic mass, but not tributary to the frame; the loads on this column are significant for the perimeter frames.

Fig. 1 shows the results of static pushover analysis for the buildings of interest, demonstrating that decreased R-factors increase design base shear and subsequent lateral strength capacity for a structure. The overstrength ratio of the structures, corresponding to pushover-estimated maximum base shear divided by design base shear, ranges from 2.3 (R = 4) to 4.1 (R = 12) for the space frames and from 1.6 to 1.8 (for R = 8 and R = 12, respectively) for the perimeter frames. Larger overstrengths are associated with the space frame buildings due to the additional strength from the gravity load design, which becomes more significant when lateral loads are relatively smaller. Perimeter frames also have a larger tributary seismic mass increasing P-Δ effects and contributing to post-yield negative stiffness. All the buildings have similar deformation capacities (presented in Table 1), as indicated by the maximum interstory drift ratio at which the negative slope of the pushover begins. As a result, differences in collapse capacity and residual capacity are primarily due to strength.

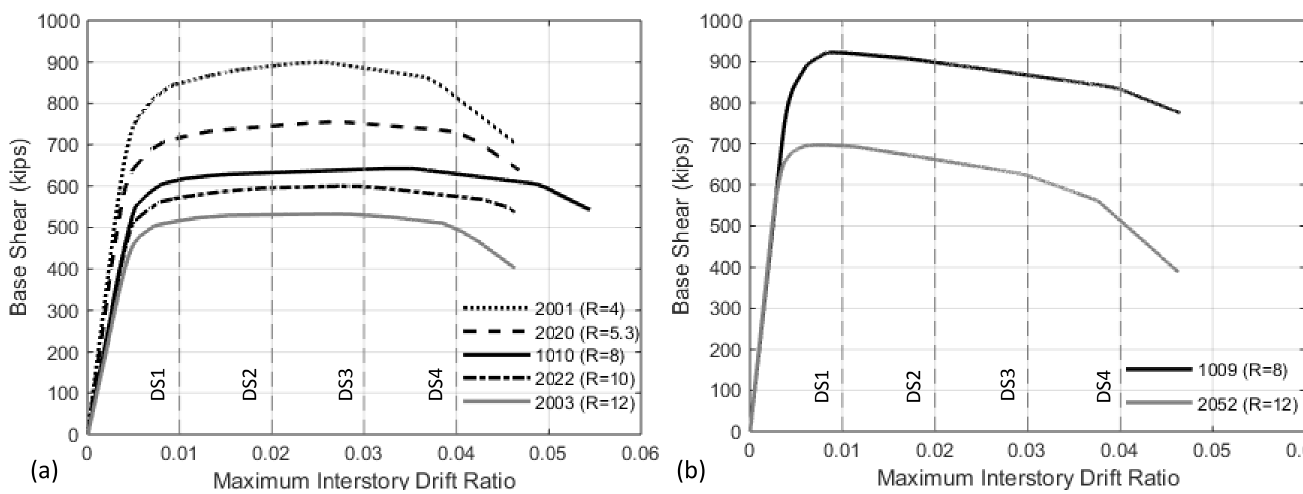

Fig. 1 – Results of static pushover analysis for RC frame buildings of interest, showing increase in strength for buildings designed for lower R-factors, and vice versa for: (a) space frames and (b) perimeter frames. This figure also illustrates the damage states considered in the assessment of residual capacity for earthquake-damaged buildings.

4. Procedure for dynamic analysis of intact and post-earthquake damaged buildings

Each of the building simulation models is subjected to a suite of 30 recorded ground motions for dynamic analysis. The ground motions used were compiled by Vamvatsikos and Cornell [12], and consist of records at firm sites from California earthquakes with magnitude ranging from 6.5 to 6.9 and with rupture distances ranging from 15-33 km. These ground motions records are considered representative of the type of ground motions expected to occur in southern California, and are used to assess the capacity of each building in its intact (undamaged) state and post-earthquake (earthquake-damaged) states. Although there is some evidence that the frequency content of an aftershock may be systematically different than the first earthquake shaking (or mainshock) the structure experiences [18], this effect was not considered in ground motion selection.

The dynamic analysis procedure employs incremental dynamic analysis (IDA) of intact buildings and post-earthquake damaged buildings using the approach described in Raghunandan *et al.* [4]. In IDA, a ground motion is applied to the nonlinear model of a building and its dynamic response is simulated and recorded. The same ground motion is then scaled and applied to the structure again and the new response is recorded. The process of scaling the ground motion and recording responses is repeated for higher intensities of ground motions until the structure collapses. Here, the ground motion intensity is quantified using spectral acceleration of ground motion at the fundamental period of the structure, $Sa(T_1)$.[1] For the buildings considered in this study, sidesway failure is the primary collapse mechanism, since column shear failures, joint shear failures and other brittle mechanisms are not expected, given that these structures are designed according to modern detailing requirements and capacity design rules [1]. Sidesway collapse is identified during the analysis if interstory drifts exceed 12%.

In dynamic analysis for an intact building, IDA is conducted for a model of the intact building with 30 ground motion records. Fig. 2(a) illustrates the results for IDA of the intact 4-story space frame model designed with R = 8 (code-conforming case). Each line in the figure presents how the structural response, measured in terms of the peak story drift ratio, varies with increasing intensities of shaking for each ground motion. The blue line on the plot highlights an example of IDA results for a single motion. The collapse capacity for a particular ground motion is the intensity of the scaled record that causes structural collapse, and corresponds to a flatlining of the IDA curve. Here, we quantify the distribution of collapse capacity for the intact buildings based on the IDA results for 30 ground to consider the influence of record to record variability on the structural response.

The IDA procedure for damaged buildings is slightly different from that of the IDA for intact buildings. In this approach, the building model is subjected to an earthquake sequence that consists of two scaled ground motions. The first ground motion in the sequence is applied to the intact building, and scaled to simulate a particular level of damage (also called a "damage state") in the model. Next, the second ground motion is scaled to evaluate the response of the model once it has entered that particular damage state. To assess the residual capacity of a damaged building using IDA, we consider all possible combinations of the 30 ground motions as the first and second parts of the sequence. The damaged-building IDA phase is carried out for 900 such earthquake sequences, whereby one ground motion record is used to simulate a particular level of earthquake damage, while the second ground motion is scaled to increasingly higher intensities until collapse is observed in the already-damaged building. Through this approach, the ground motion intensity of the scaled second ground motion in the sequence quantifies the collapse capacity of the damaged building for a particular ground motion.

In this study, four damage states are considered. The different damage states are quantified by the peak interstory drift ratio experienced by the intact structure during ground shaking in the first motion of the sequence. To simulate varying levels of damage, from fairly low to severe damage, a wide range of maximum interstory drift ratios are considered, as shown in Fig. 1: 1% (DS1), 2% (DS2), 3% (DS3) and 4% (DS4). Thus, in Damage State (DS) 1 the building experiences a peak interstory drift demand of 1% during the first motion of the sequence, before being analyzed under this damage condition in the second motion, and similarly for the other damage states. Fig. 2(b) illustrates the IDA results for the DS4 damaged 4-story building designed with R = 8. In this figure, the x-axis indicates the maximum interstory drift experienced by the building during the entire two motion sequence, and the y-axis indicates the intensity of the second ground motion in the sequence. Therefore, for each IDA curve (*e,g.* the blue line in Fig. 2(b)) the maximum interstory drift for the structure during the entire earthquake sequence (x-axis), at low intensities of the second ground motion, is governed by the drift in the first motion in the sequence, in this case around 4%.[2] Fig. 2(b) shows the reduced collapse capacity of the as-damaged building compared to the intact building.

In total, this study requires analysis of 7 buildings x 4 damage states x 900 sequences for a total of 25,200 ground motion sequences to quantify residual capacity. The evaluation of a building's residual strength is a computationally intensive process, necessitating the use of parallel processing on a high-performance supercomputer.

[1] Note that each of the buildings has a slightly different period, T_1. However, the space frame buildings' periods are close enough to each other to provide comparison without conversion to a common period, and similarly for the perimeter frames.

[2] The required scale factors to move an intact building into a particular damage state are estimated from linear interpolation of the intact building IDA curves. As a result, the maximum interstory drift varies between 3.5%-4.5% during the first scaled earthquake in the sequence even though the defined damage state corresponds to 4% drift.

5. Assessments of Residual Capacity

5.1 Collapse capacity of intact buildings

Building collapse performance is characterized using collapse fragility curves. A collapse fragility curve quantifies the probability of collapse for a building at a particular level of ground motion intensity, as obtained from statistics of the IDA results, assuming a lognormal collapse capacity distribution from the individual motions. The collapse fragilities (quantified in terms of $Sa(T_1)$) for all buildings in the intact state are presented in Fig. 3. The median collapse capacities, defined as the intensity of ground motion that corresponds to a 50% probability of building collapse, are summarized in Table 2 and Table 3. As expected, the stronger buildings (R < 8) have larger median collapse capacities than the weaker code-minimum and non-code compliant frames.

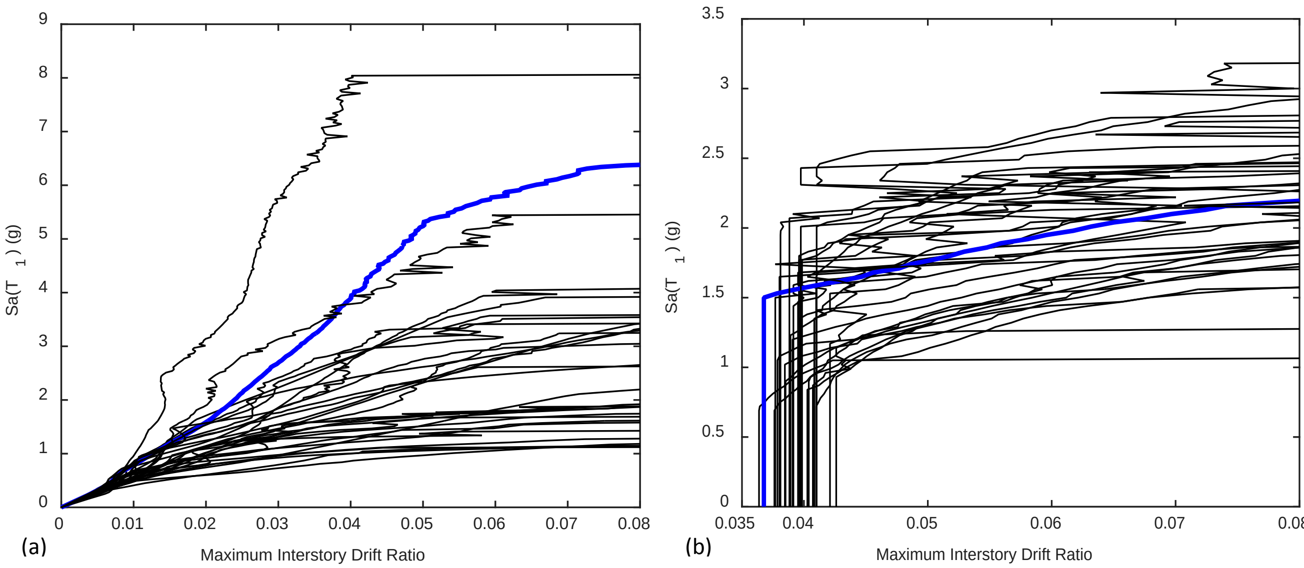

Fig. 2 – Incremental dynamic analysis results for four-story (ID 1010, R = 8) evaluated as: (a) intact building (30 ground motions) and (b) DS4 damaged building (30 earthquake sequences with the same second ground motion and 30 different first ground motions simulating DS4 damage state).

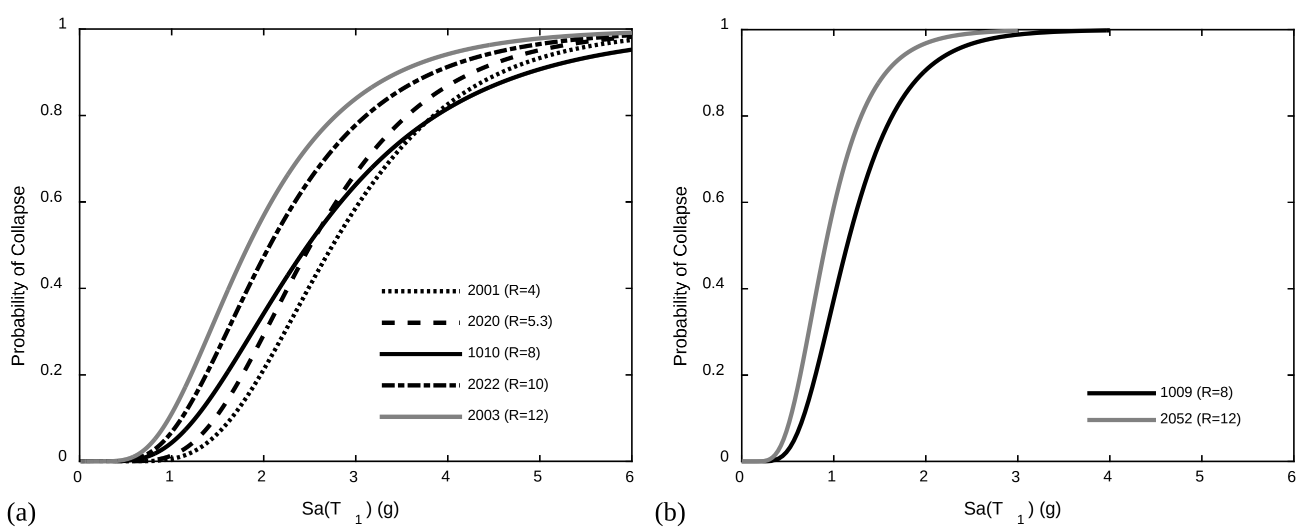

Fig. 3 – Collapse fragility curves for intact buildings designed with different strengths for: (a) space frames and (b) perimeter frames.

5.2 Residual capacity of earthquake-damaged buildings

The collapse capacity of an earthquake-damaged building, as assessed through the sequenced IDA procedure, represents a measure of its residual collapse capacity. Table 2 and Table 3 report the median residual capacities for each of the buildings, under all four of the damage states considered. As expected, the more severe the seismic damage in the building, as represented by the damage state, the lower the residual capacity of the damaged building. This trend is exhibited in all of the buildings assessed, regardless of design strength level. Indeed, in relative terms, the impact of damage is almost equivalent among the group of buildings in that the first damage state reduces the collapse capacity by about 7%, the second by 18% etc. This symmetry in impact is possibly due to the fact that for all damage states considered every building has entered the nonlinear range of structural response (see Fig. 1), thus causing benefits of additional design strength to persist in an absolute but not relative sense. The perimeter frame buildings (Table 3) show somewhat less degradation in capacity relative to the original collapse capacities likely due to P-Δ effects, which, along with ground motion intensity and frequency content, are significant drivers of collapse for these buildings. In U.S. design standards [13], 2% drift is the maximum allowable drift under design seismic loading. At this level of transient drift (DS2), the space frames possess about an 18% lower collapse capacity than their undamaged counterparts. In other words, the residual collapse capacity is 18% lower than the intact building collapse capacity suggesting that, should this level of shaking occur, the building could incur a reduction in collapse capacity on the order of one-fifth of its initial, undamaged capacity.

The influence of lateral strength on residual capacity is plotted in Fig. 4. As expected, the buildings designed for the highest lateral forces (lowest R) are stronger than those designed for lower seismic design levels (higher R). This trend applies to the intact buildings, but also to the residual capacity of the earthquake-damaged buildings. In other words, the strongest buildings remain stronger, even when they have experienced the same level of damage as the weaker buildings. Therefore, increasing lateral strength at the design stage *(i.e.* using a lower R value) can help to ensure sufficient residual capacity after a building is subjected to earthquake shaking. However, the amount to which lateral strength should be increased upfront depends on the desired level of residual capacity for a structure to maintain after experiencing damage and the level of damage considered.

Table 2 – Collapse capacities and residual capacities for space frame buildings.

Building ID	**R**	**Median collapse capacity, Sa(T_1) (g)**					**% Reduction in collapse capacity from intact building**			
		Intact	**DS1**	**DS2**	**DS3**	**DS4**	**DS1**	**DS2**	**DS3**	**DS4**
2001 - strongest	4	2.75	2.60	2.28	1.99	1.68	-5.4%	-17.1%	-27.5%	-39.1%
2020	5.3	2.51	2.29	2.01	1.78	1.41	-8.6%	-20.0%	-29.2%	-43.7%
1010	8	2.48	2.33	2.06	1.86	1.59	-6.2%	-16.9%	-25.1%	-35.9%
2022	10	2.07	1.90	1.68	1.51	1.27	-8.1%	-18.9%	-27.2%	-38.5%
2003-weakest	12	1.84	1.70	1.50	1.36	1.18	-7.2%	-18.1%	-26.1%	-35.6%

To consider what a given level of design strength produces in terms of residual capacity, consider the case where the stronger and weaker buildings are subjected to the same intensity ground motion. For this intensity of shaking, the stronger building will experience less drift, *i.e.* less damage. Therefore, stronger buildings will experience a lower percentage reduction in their residual capacity to withstand subsequent shaking. To illustrate this point, Table 4 summarizes the mean maximum interstory drift ratio experienced by buildings at two levels of shaking, (a) Sa(T_1) = 0.62g (which is approximately equal to S_{D1} value at the site of interest), and, Sa(T_1) = 0.9g (which is approximately equal to S_{M1} value at the site). For the same intensity of shaking, the stronger buildings (low design R values), incur less damage (lower maximum interstory drift ratios) as compared to the weaker buildings (high design R values). For example, the R = 4 space frame experiences a mean drift of 1.3% at S_{M1} as compared to the code-conforming (R = 8) building, which experiences 1.8% drift at that intensity of shaking.

Therefore, at S_{M1} intensity shaking, the stronger building is in (approximately) DS1, whereas the weaker building is in (approximately) DS2. As a result, the weaker damaged building has a 17% decrease in residual capacity compared to the weaker intact building (2.06g from 2.48g). The stronger, code-compliant, building sees around 6% reduction in collapse capacity (from its intact collapse capacity down to 2.60g). Thus, the stronger building demonstrates better performance due to its superior (reduced) drifts in the first motion, which correspond to less damage, and subsequently higher residual capacity. As a result, the R = 4 building damaged under S_{M1} intensity shaking has the same seismic collapse resistance as the intact R = 8 code-conforming building.

Table 3 – Collapse capacities and residual capacities for perimeter frame buildings.

Building ID	**R**	**Median collapse capacity, Sa(T_1) (g)**					**% Reduction in collapse capacity from intact building**			
		Intact	**DS1**	**DS2**	**DS3**	**DS4**	**DS1**	**DS2**	**DS3**	**DS4**
1009 - stronger	8	1.33	1.30	1.19	1.16	-1.0	-2.1%	-10.1%	-13.0%	-22.9%
2052 - weaker	12	1.05	1.02	0.93	0.82	0.7	-2.3%	-11.4%	-21.1%	-37.0%

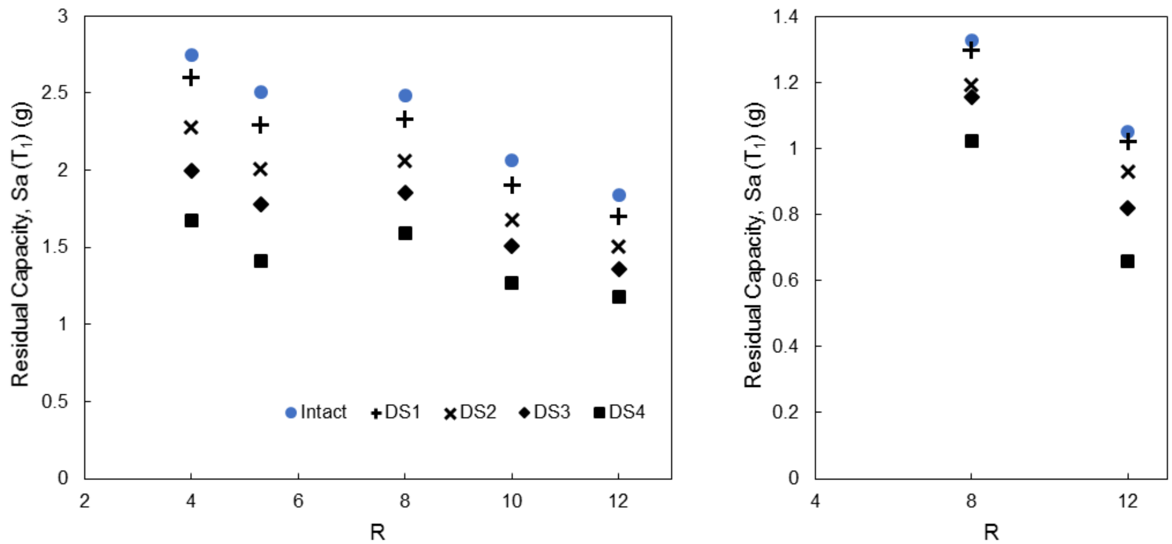

Fig. 4 – Residual capacity vs. R (inverse of design strength) for intact buildings and earthquake-damaged buildings considering four damage states, for (a) space frames and (b) perimeter frames.

Table 4 – Mean maximum drift[1] experienced by space and perimeter frames for intensity of shaking approximately equal to code-defined design S_{D1} and maximum considered earthquake (MCE) S_{M1} values.

Space Frames				**Perimeter Frames**			
Building ID	**R**	**Mean Max. Interstory Drift**		**Building ID**	**R**	**Mean Max. Interstory Drift**	
		S_{D1} Sa(T_1)=0.6g	**S_{M1} Sa(T_1)=0.9g**			**S_{D1} Sa(T_1)=0.6g**	**S_{M1} Sa(T_1)=0.9g**
2001	4	0.9%	1.3%	1009	8	2.2%	3.4%
2020	5.3	0.9%	1.4%	2052	12	2.6%	4.2%
1010	8	1.1%	1.8%				
2022	10	1.3%	2.4%				
2003	12	1.5%	2.6%				

[1] Mean drifts computed only from ground motions in which the building did not collapse.

6. Conclusions

This study quantifies the impact of design lateral strength on the residual collapse capacity of a structure. The results are based on incremental dynamic analysis of seven buildings with varying strengths, subjected to a suite of ground motion sequences. Results show that buildings designed for the highest lateral forces have greater capacity to resist collapse than those designed for lower seismic design levels. Both intact and earthquake-damaged buildings demonstrate this trend, showing that the strongest (above code) buildings remain stronger, even when they have experienced the same level of damage as the weaker buildings. Moreover, findings suggest that stronger buildings will experience a lower percentage reduction in residual capacity for the same level of mainshock shaking than will code-minimum or weaker buildings.

The results of this study imply that design strength can be adjusted to improve post-earthquake outcomes. Specifically, increasing lateral strength at the design stage (*i.e.* using lower a R value in U.S. design) can help to ensure sufficient residual strength in the structure after it is subjected to ground shaking. As a result, increasing lateral strength may allow a building that previously would have been demolished after a mainshock event instead to be repaired. This change could decrease post-earthquake losses and enhance resilience by potentially allowing communities to regain a level of normalcy sooner after an earthquake event. However, the amount to which lateral strength should be increased upfront depends on the desired level of residual capacity for a structure to maintain after experiencing damage from a single earthquake shaking event. Future work could investigate what changes in structural design are required to achieve a desired level of residual capacity after a particular damage state in a mainshock event, *i.e.* designing in reverse to meet a specific residual capacity. The results from this study can also help to assess how the residual capacity of reinforced concrete frames with lateral strength lower than the code requirements will vary for different levels of earthquake damage. This is important for building policy decision-making in places where design values (*e.g.* the Pacific Northwest region of the U.S.) have increased significantly.

8. Acknowledgments

This analysis utilizes the Janus supercomputer, which is supported by the National Science Foundation (Award #CNS-0821794), the University of Colorado Boulder, the University of Colorado Denver, and the National Center for Atmospheric Research. The Janus supercomputer is operated by the University of Colorado Boulder. Any use of trade, firm, or product names is for descriptive purposes only and does not imply endorsement by the U.S. Government The authors gratefully acknowledge the assistance of Joseph Kasprzyk and Travis Marcilla in installing *OpenSees* on the supercomputer.

8. References

[1] C. B. Haselton, A. B. Liel, G. G. Deierlein, B. S. Dean, and J. H. Chou, "Seismic collapse safety of reinforced concrete buildings. I: Assessment of ductile moment frames," *Journal of Structural Engineering*, vol. 137, no. 4, pp. 481–491, 2011.

[2] S. Welsh-Huggins and A. B. Liel, "Is a Stronger Building also Greener? Influence of Seismic Design Decisions on Building Life-Cycle Economic and Environmental Impacts," 2016.

[3] N. Nazari, J. W. van de Lindt, and Y. Li, "Effect of Mainshock-Aftershock Sequences on Woodframe Building Damage Fragilities," *Journal of Performance of Constructed Facilities*, vol. 29, no. 1, p. 04014036, 2015.

[4] M. Raghunandan, A. B. Liel, and N. Luco, "Aftershock collapse vulnerability assessment of reinforced concrete frame structures," *Earthquake Engineering & Structural Dynamics*, vol. 44, no. 3, pp. 419–439, 2015.

[5] R. Han, Y. Li, and J. van de Lindt, "Assessment of Seismic Performance of Buildings with Incorporation of Aftershocks," *Journal of Performance of Constructed Facilities*, vol. 29, no. 3, p. 04014088, 2015.

[6] A. ATC, "20: Procedures for Postearthquake Safety Evaluation of Buildings," *Applied Technology Council, San Francisco*, 1989.

[7] New Zealand Society for Earthquake Engineering, "Building afety evaluation in a state of emergency: guidelines for territorial authorities," Aug. 2009.

[8] A. B. Liel, R. B. Corotis, G. Camata, J. Sutton, R. Holtzman, and E. Spacone, "Perceptions of Decision-Making Roles and Priorities That Affect Rebuilding after Disaster: The Example of L'Aquila, Italy," *Earthquake Spectra*, vol. 29, no. 3, pp. 843–868, 2013.

[9] G. L. Yeo and C. A. Cornell, "Building tagging criteria based on aftershock PSHA," in *Proceeding of the 13WCEE, Vancouver, Canada. Paper*, 2004.

[10] F. Marquis, J. J. Kim, K. J. Elwood, and S. E. Chang, "Understanding post-earthquake decisions on multi-storey concrete buildings in Christchurch, New Zealand," *Bulletin of Earthquake Engineering*, pp. 1–28, 2015.

[11] C. B. Haselton and G. G. Deierlein, "Assessing seismic collapse safety of modern reinforced concrete moment frame buildings," Blume Center Stanford University, 159, 2006.

[12] D. Vamvatsikos and C. A. Cornell, "Incremental dynamic analysis," *Earthquake Engineering & Structural Dynamics*, vol. 31, no. 3, pp. 491–514, 2002.

[13] ASCE (American Society of Civil Engineers), *Minimum Design Loads for Buildings and Other Structures: ASCE Standard 7-10*. Reston, VA: ASCE Publications, 2010.

[14] FEMA, *Recommended methodology for quantification of building system performance and response parameters (FEMA P-695)*. Prepared by the Applied Technology Council for FEMA, 2009.

[15] PEER, "OpenSEES." 2013.

[16] L. F. Ibarra, R. A. Medina, and H. Krawinkler, "Hysteretic models that incorporate strength and stiffness deterioration," *Earthquake engineering & structural dynamics*, vol. 34, no. 12, pp. 1489–1511, 2005.

[17] C. B. Haselton, *Beam-column element model calibrated for predicting flexural response leading to global collapse of RC frame buildings*. Pacific Earthquake Engineering Research Center, 2008.

[18] J. Ruiz-García, "Mainshock-aftershock ground motion features and their influence in building's seismic response," *Journal of Earthquake Engineering*, vol. 16, no. 5, pp. 719–737, 2012.